



## Spectral analysis and quantum chemical calculations of 4-(2-keto-1-benzimidazoliny) piperidine

M.Boopathi<sup>1,2</sup>, P. Udhayakala<sup>2\*</sup>, G. R. Ramkumaar<sup>3</sup> and T. S. Renuga Devi<sup>4</sup>

<sup>1</sup>Department of physics, Pachaiyappa's College for Men, Kanchipuram- 631501, India

<sup>2</sup>Department of Chemistry, Dr. M. G. R. Educational and Research Institute, Chennai -600095, India

<sup>3</sup>Department of Physics, C. Kandaswami Naidu College for Men, Chennai, India

<sup>4</sup>Department of Physics, Women's Christian College, College Road, Chennai, India

---

### ABSTRACT

*In the present study, we have compared the experimentally observed spectral data FT-IR and FT-Raman of the title compound 4-(2-Keto-1-benzimidazoliny) piperidine (KBP) with the spectral data obtained by DFT/B3LYP method using 6-311++G(d,p) basis set. <sup>1</sup>H and <sup>13</sup>C NMR chemical shifts were calculated by using gauge including atomic orbital (GIAO) method and compared with experimental data obtained. The electrophilic and nucleophilic reactivity regions were shown using a molecular electrostatic potential (MEP) map. From the frontier molecular orbital energies (HOMO-LUMO), global reactivity descriptors have been derived. Local reactivity descriptor such as Fukui functions were calculated to explain the reactivity site of the atoms within the molecule.*

**Keywords:** 4-(2-keto-1-benzimidazoliny)piperidine, spectroscopic, HOMO-LUMO and Fukui function.

---

### INTRODUCTION

Piperidine and their derivatives play a key role as pharmacophore in the pharmaceutically active molecules, naturally occurring alkaloids, pharmaceuticals, agrochemicals and as synthetic intermediates with interesting biological, physical and pharmacological properties[1-4]. The piperidine moieties are the key structural component of successful anti-parkinson's drugs[5] and in many cardiovascular drugs[6]. Therapeutically active agents containing piperidine ring as essential part are well known for their analgesic, anti-inflammatory, antidepressant, antipsychotic, antiviral, antimicrobial, agonistic, and antagonistic activities [7]. In recent years density functional theory (DFT) has become a powerful tool in the investigation of molecular structures and vibrational spectra, especially B3LYP method has been widely used [8,9]. Several workers have investigated structural, vibrational spectroscopic and adsorption studies of piperidine derivatives using experimental and DFT methods [10-12]. In the present investigation, a detailed vibrational analysis based on FT-IR, FT-Raman and NMR spectra of the title molecule is compared with the gas phase theoretical calculation data obtained by DFT/B3LYP method. The molecular properties like global reactivity descriptors, molecular electrostatic potential surface have been calculated to get a better insight of the properties of the title molecule. Local reactivity descriptors like Fukui functions, local softness have been computed to predict reactivity and reactive sites on the molecule.

### MATERIALS AND METHODS

#### Experimental details

The compound 4-(2-keto-1-benzimidazoliny) piperidine (KBP) was obtained from Sigma-Aldrich chemicals, U.S.A with a stated purity of greater than 98% and used as such without further purification. The FT-IR spectrum of the compound was recorded in the region 4000-400cm<sup>-1</sup> on a Perkin Elmer FT-IR Spectrophotometer. The FT-Raman spectrum was recorded in the Bruker FRA 106/S instrument equipped with Nd:YAG laser source operating

at 1064 nm line widths in the range of 3500–50cm<sup>-1</sup>. The spectral measurements were carried out at Sophisticated Analytical Instrument Facility, IIT, Chennai, India.

### Computational details

The entire quantum chemical calculations have been performed by using DFT/B3LYP level of theory with standard basis set 6-311++G(d,p) using Gaussian 09W [13] program package, invoking gradient geometry optimization [14]. In order to fit the theoretical wavenumbers to the experimental, the computed harmonic frequencies were scaled by 0.981 for frequencies less than 1700cm<sup>-1</sup> and 0.9615 for higher frequencies [15]. The chemical shifts of proton and carbon NMR were calculated with gauge including atomic orbital (GIAO) approach [16] by applying B3LYP/6-311++G(d,p) method of the title compound and compared with the experimental NMR spectra. The theoretical <sup>1</sup>H and <sup>13</sup>C NMR chemical shift values were obtained using the GIAO calculation [17]. To visualize variably charged regions of a molecule in terms of colour grading the molecular electrostatic potential (MEP) map have been plotted. The global reactivity descriptors like global hardness ( $\eta$ ), global softness ( $S$ ), electronegativity ( $\chi$ ), chemical potential ( $\mu$ ) and electrophilicity index ( $\omega$ ) have been calculated from the value of highest occupied molecular orbital (HOMO) and lowest unoccupied molecular orbital (LUMO). The local reactivity has been analyzed by means of the Fukui function.

## RESULTS AND DISCUSSION

### Molecular geometry

The molecule under investigation consists of two rings one benzimidazoliny (b-ring) and another piperidine (p-ring). The geometry of the title molecule is considered to have C<sub>1</sub> point group symmetry. The optimized molecular structure along with the numbering of atoms of 4-(2-keto-1-benzimidazoliny) piperidine (KBP), obtained from GaussView program is shown in Fig.1. The global minimum energy obtained by the DFT/ B3LYP/6-311++G(d,p) for the optimized structure of the title compound is -705.8043 a.u.

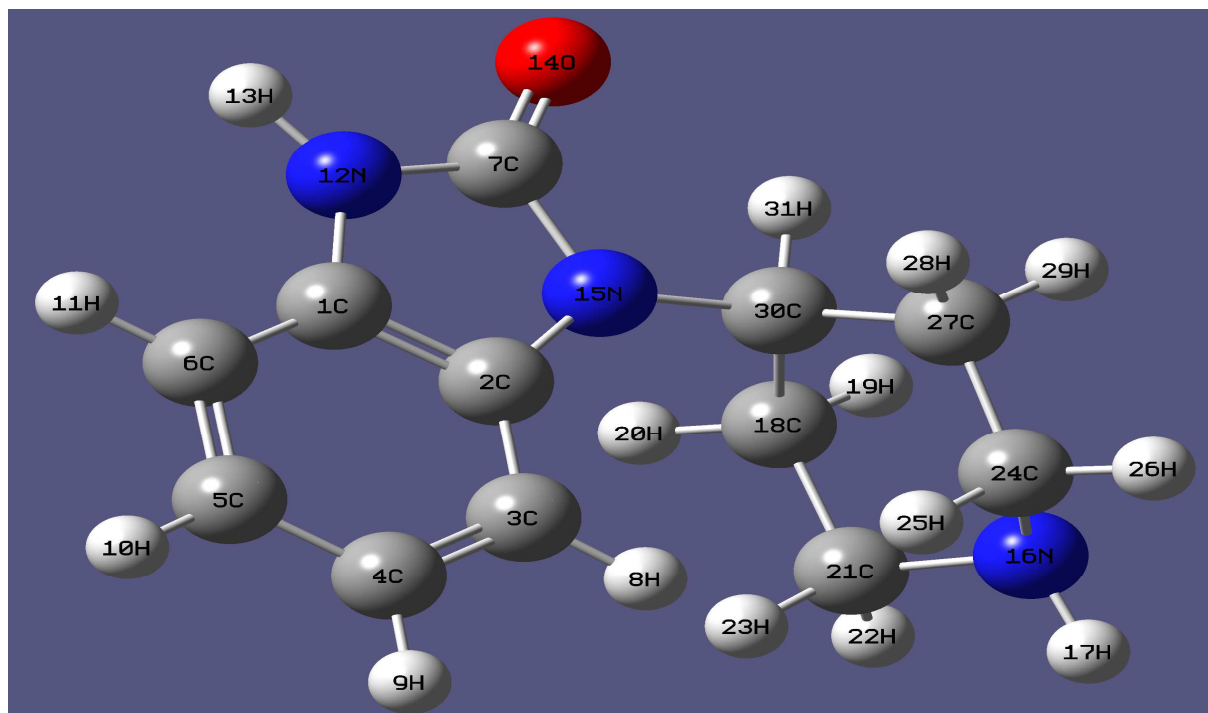


Fig.1 Optimized structure and atoms numbering of 4-(2-keto-1-benzimidazoliny) piperidine (KBP)

### Vibrational spectral analysis

The objective of the vibrational analysis is to find the vibrational modes connected with the molecular structure of the title compound. The studied molecule consists of 31 atoms having 87 modes of vibration and most of the modes are active in both IR and Raman spectra. The calculated vibrational wavenumbers are compared with the experimental FT-IR and FT-Raman frequencies and listed in table 1. The calculated and experimental FT-IR, FT-Raman spectra are shown in Figs. 2 and 3 respectively.

### C-H vibrations

In the present study, there are two types of C-H modes; C-H modes in the benzimidazoliny ring (b-ring) and the C-H modes in the piperidine ring (p-ring). Usually, the C-H bands in the aromatic rings are found to be weak due to the decrease in the dipole moment caused by the reduction of negative charge on the carbon atoms. The C-H stretching modes of the b-ring were predicted in the range 2931-2994 $\text{cm}^{-1}$ . The C-H stretching vibrations for the title molecule is observed as a very strong band at 2935, 2947 and 2962 $\text{cm}^{-1}$  in FT-IR and 2942, 2948, 2951 and 2995 $\text{cm}^{-1}$  in FT-Raman spectra. The theoretically computed wavenumbers at 2931, 2940, 2952 and 2994 $\text{cm}^{-1}$  show good agreement with the recorded spectra and the literature data [18]. The C-H stretching vibration in the (P-ring) of the title molecule are observed at 2737, 2818, 2838 and 2860 $\text{cm}^{-1}$  in FT-IR and 2731, 2736, 2827, 2839 and 2860 $\text{cm}^{-1}$  in FT-Raman spectra. The theoretically calculated wavenumbers at 2728, 2733, 2826, 2828 and 2860 $\text{cm}^{-1}$  show good agreement with the experimental observations. The literature value also supports this [19]. The C-H in-plane bending vibrations generally occurs in the region 1300-1000 $\text{cm}^{-1}$  [20]. The C-H in-plane bending modes of vibrations are assigned at 1005, 1063, 1103, 1137, 1150 and 1365 $\text{cm}^{-1}$  in the theoretically calculated value is good in agreement with the experimental bands at 1017, 1064, 1127 and 1365 $\text{cm}^{-1}$  in FT-IR and 1006, 1065, 1103, 1136, 1153 and 1372 $\text{cm}^{-1}$  in FT-Raman spectra. Bands involving the C-H out-of-plane bending vibrations appear in the range 1000-675  $\text{cm}^{-1}$  [21]. The bands at 814, 913 and 925 $\text{cm}^{-1}$  in FT-IR spectrum and 816, 882 and 934 $\text{cm}^{-1}$  in FT-Raman spectrum are assigned to C-H out-of-plane bending mode of vibrations. The theoretically calculated values at 815, 884 and 930 $\text{cm}^{-1}$  are in correlation with the experimental observations.

### C-C vibrations

The C-C stretching modes of the pyridine are expected in the range 1650-1100 $\text{cm}^{-1}$  which are not significantly influenced by the nature of the substituents [22]. In the present study, the wavenumbers observed at 1110, 1322, 1451 and 1605 $\text{cm}^{-1}$  in the FT-IR 1102, 1307, 1459, 1576 and 1604  $\text{cm}^{-1}$  in FT-Raman spectra are assigned to C-C stretching vibrations. The theoretically computed values at 1101, 1301, 1449, 1574 and 1597 $\text{cm}^{-1}$  show an excellent agreement with experimental data. The very strong band observed at 945 $\text{cm}^{-1}$  in the FT-Raman spectrum of the title molecule have been assigned to ring-breathing vibration. The theoretically predicted wavenumber at 944 $\text{cm}^{-1}$  is good agreement with the experimental observation. The theoretically predicted wavenumbers at 287, 562 and 722 $\text{cm}^{-1}$  are assigned to C-C out-of-plane bending vibrations. These findings are well in line with the experimental bands observed at 544 and 742 $\text{cm}^{-1}$  in FT-IR and 289, 563 and 725 $\text{cm}^{-1}$  in FT-Raman spectrum. The bands observed at 689 $\text{cm}^{-1}$  in both FT-IR and FT-Raman spectra have been assigned to C-C in-plane bending vibrations. The calculated wavenumber at 689 $\text{cm}^{-1}$  is excellent agreement with the experimental data.

### CH<sub>2</sub> Vibrations

The high frequency stretching modes assignments can be made on the basis of their relative intensity. One can expect six fundamental assignments to be associated to each CH<sub>2</sub> group. They are CH<sub>2</sub> stretching (symmetric and asymmetric), CH<sub>2</sub> scissoring, CH<sub>2</sub> rocking, CH<sub>2</sub> wagging and CH<sub>2</sub> twisting mode of vibration. Generally the C-H stretching vibration of methylene group are at lower frequencies than those of aromatic C-H ring stretching [23]. For non-planar molecules, the asymmetric stretching mode is much more intense than the symmetric stretching mode of vibration. Generally, the CH<sub>2</sub> asymmetric and symmetric stretching vibrations of methylene group observed in the region 3000-2900 $\text{cm}^{-1}$  and 2900-2800 $\text{cm}^{-1}$  [24]. In the title molecule, a strong band observed at 2852 $\text{cm}^{-1}$  in FT-IR and 2842, 2848 $\text{cm}^{-1}$  in FT-Raman spectra are assigned to CH<sub>2</sub> asymmetric stretching mode of vibration. The computed values at 2847 and 2848 $\text{cm}^{-1}$  are well agreed with the experimental observations. The CH<sub>2</sub> symmetric stretching vibrations are observed at 2797 and 2808 $\text{cm}^{-1}$  in FT-IR and 2805, 2809 $\text{cm}^{-1}$  in FT-Raman spectra having well agreement with the theoretically calculated value by B3LYP method at 2805, 2807 $\text{cm}^{-1}$ . The computed wavenumber at 1466 $\text{cm}^{-1}$  is well agreed with the experimental observations at 1478 $\text{cm}^{-1}$  in FT-IR and 1489 $\text{cm}^{-1}$  FT-Raman spectra which is assigned to CH<sub>2</sub> scissoring mode of vibration. A strong band at 1378 $\text{cm}^{-1}$  in FT-Raman spectra is assigned to CH<sub>2</sub> wagging. The calculated wavenumber at 1371 $\text{cm}^{-1}$  is well agreed with the observed one. This is also supported by the literature value [25]. The bands observed at 1191, 1171 $\text{cm}^{-1}$  in FT-IR and FT-Raman spectra is assigned to CH<sub>2</sub> twisting mode, which is in correlation with the calculated value at 1168 $\text{cm}^{-1}$ . The experimental observations at 980 $\text{cm}^{-1}$  in FT-IR and 997 $\text{cm}^{-1}$  in FT-Raman spectra are assigned to CH<sub>2</sub> rocking mode. This is in line with the calculated value at 992 $\text{cm}^{-1}$ .

### C-N Vibrations

The C-N stretching vibration usually lies in the region 1200 to 1400  $\text{cm}^{-1}$  [26]. The identification of this vibrations is a task, since in this region mixing of several bands are possible. In the title molecule, the band observed at 1310 $\text{cm}^{-1}$  in FT-Raman spectra have been assigned to C-N stretching vibration. The theoretically computed value at 1302 $\text{cm}^{-1}$  is well correlated with the experimental observations and literature data [27]. C-N in-plane and out-of-plane bending mode vibration of the title molecule are assigned at 544 $\text{cm}^{-1}$  in FT-IR and 563, 203  $\text{cm}^{-1}$  in FT-Raman spectra. The calculated value at 562, 206 $\text{cm}^{-1}$  is well aligned with the experimental wavenumbers as well as the values reported in the literature [28].

**N-H Vibrations**

The N-H stretching vibrations are observed strongly in the region  $3390 \pm 60 \text{ cm}^{-1}$  [29]. The title compound contains 2 N-H attachments. One in the benzimidazolanyl ring (b-ring) and the other in the piperidine ring (p-ring). In this study, the strong band at  $3392 \text{ cm}^{-1}$  in FT-IR and  $3397 \text{ cm}^{-1}$  in FT-Raman spectra are assigned to N-H stretching vibration in b-ring. The computed value for this vibration found at  $3395 \text{ cm}^{-1}$ . The same is observed at  $3256 \text{ cm}^{-1}$  in FT-IR and  $3274 \text{ cm}^{-1}$  in FT-Raman spectra in p-ring. The theoretically calculated value for this vibration obtained at  $3270 \text{ cm}^{-1}$ .

**C=O vibrations**

The characteristic frequency of carbonyl group has been extensively used to study in wide range of different classes of compounds. A strong absorption band observed in these compounds due to C=O stretching vibration is observed in the region  $1750\text{-}1600 \text{ cm}^{-1}$  [30]. If a carbonyl group is part of a conjugated system, then the wavenumber of the carbonyl stretching vibration decreases, the reason being that the double bond character of the C=O group is less due to the  $\pi$ -electron conjugation being localized. For the title compound, the C=O stretching vibrational mode is observed as a strong band at  $1619 \text{ cm}^{-1}$  in FT-IR,  $1649 \text{ cm}^{-1}$  in FT-Raman and the corresponding DFT calculation give this mode at  $1649 \text{ cm}^{-1}$ . The band observed at  $610 \text{ cm}^{-1}$  in FT-IR and  $588 \text{ cm}^{-1}$  in FT-Raman spectra are assigned to in-plane bending modes of C=O vibration. The computed value by B3LYP method at  $589 \text{ cm}^{-1}$  in agreement with the experimental observation. The out of plane bending vibrations of C=O is also observed at  $457 \text{ cm}^{-1}$  in FT-Raman which is in agreement with the computed value at  $464 \text{ cm}^{-1}$ . The present assignments are in good agreement with the literature values [31,32].

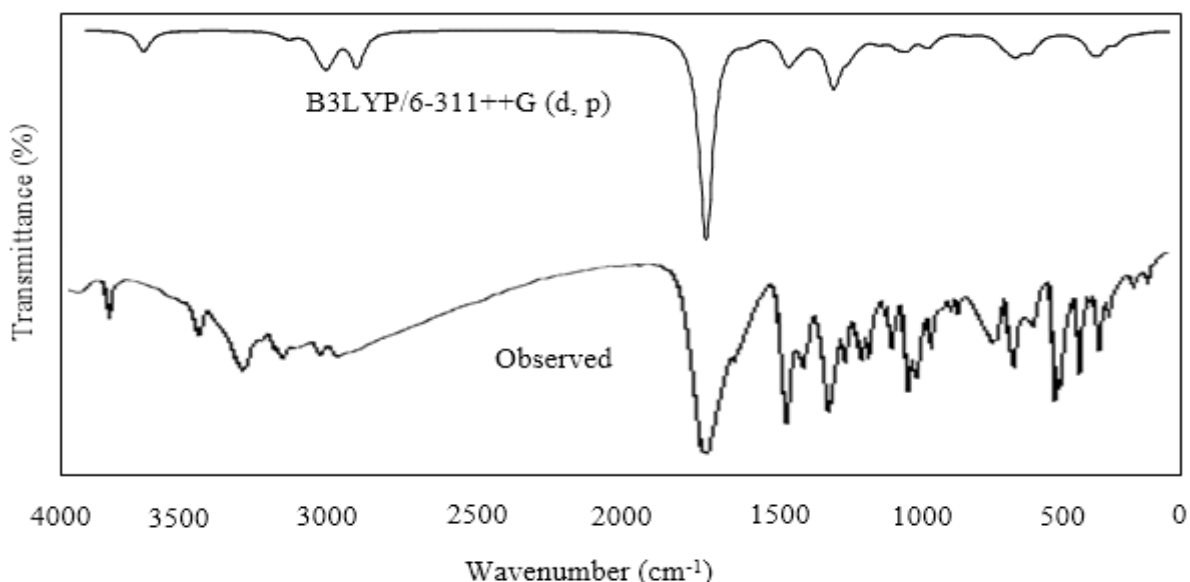


Fig.2 Observed and calculated FT-IR spectra of 4-(2-keto-1-benzimidazolanyl) piperidine (KBP)

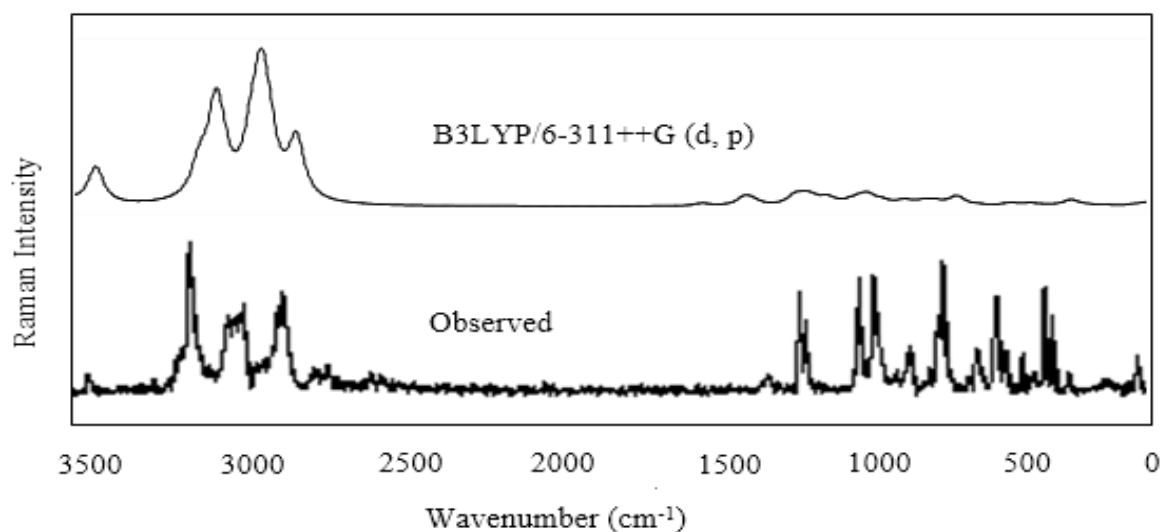


Fig.3 Observed and calculated FT-Raman spectra of 4-(2-keto-1-benzimidazolanyl) piperidine (KBP)

Table 1. Vibrational assignments of FT-IR and FT-Raman peaks along with the theoretically computed wavenumbers of 4-(2-keto-1-benzimidazoliny) piperidine (KBP)

S.No	IR	Raman	B3LYP	Vibrational Assignments
1			40	butterfly
2		69	60	t ring(b)+ $\gamma$ ring(p)
3		81	83	t ring(b)
4		130	119	$\omega$ ring(b)+ $\gamma$ C=O
5		152	147	$\omega$ ring(p)
6		203	206	$\gamma$ ring(b), $\gamma$ ring(p)+ $\gamma$ C-N
7		226	237	$\rho$ ring(p)
8		234	238	$\gamma$ C-N, $\gamma$ ring(b)+ $\gamma$ ring(p),
9		289	287	$\gamma$ ring(b)+ $\gamma$ C-C
10		324	322	$\gamma$ N-H
11		372	371	$\delta$ CH <sub>2</sub>
12		397	393	$\gamma$ N-H (b-ring)
13		413	402	$\delta$ CH <sub>2</sub>
14		444	443	$\gamma$ N-H (b-ring)
15		457	464	$\gamma$ C=O+ $\gamma$ N-H
16		474	469	$\gamma$ N-H (p-ring)+ $\rho$ CH <sub>2</sub>
17	491	482	482	ring stretching (b-ring)+ $\rho$ CH <sub>2</sub>
18	522	521	519	$\rho$ CH <sub>2</sub>
19	544	563	562	$\gamma$ C-C (b-ring)+ $\beta$ C-N
20	610	588	589	$\beta$ C=O
21	636	637	639	ring stretching (b-ring)+ $\rho$ CH <sub>2</sub>
22	662	666	666	ring breathing(p-ring)+ $\gamma$ N-H
23	689	689	689	$\beta$ C-C (b-ring)+ $\gamma$ N-H
24		712	712	$\gamma$ C-H (b-ring)
25	742	725	722	$\gamma$ C-C (b-ring)
26		731	730	$\gamma$ C-H (b-ring) + $\gamma$ C-N
27	756	755	758	$\gamma$ N-H (b-ring)
28		771	762	$\rho$ CH <sub>2</sub>
29		794	803	ring breathing (p-ring)
30	814	816	815	$\gamma$ C-H (b-ring)
31	846	855	856	ring stretching (b-ring)
32	866	858	857	ring stretching (p-ring)
33		878	876	$\nu$ C-C (p-ring)
34	913	882	884	$\gamma$ C-H (b-ring)
35	925	934	930	$\gamma$ C-H (b-ring)
36		945	944	ring breathing(b-ring)
37	980	997	992	$\delta$ C-H+ $\rho$ CH <sub>2</sub>
38		999	993	$\delta$ CH <sub>2</sub> (p-ring)
39	1017	1006	1005	$\beta$ C-H
40	1036	1024	1020	$\rho$ CH <sub>2</sub>
41	1064	1065	1063	$\nu$ C-C + $\beta$ C-H
42		1075	1074	$\omega$ CH <sub>2</sub>
43	1089	1088	1087	$\rho$ CH <sub>2</sub>
44	1110	1102	1101	$\nu$ C-C (p-ring)
45		1103	1103	$\beta$ C-H+ $\nu$ C-N
46	1127	1136	1137	$\beta$ C-H (b-ring)
47		1153	1150	$\beta$ C-H
48	1151	1153	1151	$\delta$ C-H
49	1191	1171	1168	t CH <sub>2</sub>
50	1215	1216	1215	$\beta$ C-H, $\beta$ N-H
51	1257	1246	1245	t CH <sub>2</sub>
52		1256	1255	$\beta$ C-H + $\beta$ N-H + $\nu$ C-C
53	1276	1279	1277	t CH <sub>2</sub>
54	1291	1290	1296	$\beta$ C-H (b-ring)
55	1322	1307	1301	t C-H (p-ring)+ $\nu$ C-C
56		1310	1302	$\nu$ C-N
57		1316	1308	$\omega$ C-H (p-ring)
58		1336	1333	$\omega$ CH <sub>2</sub>
59		1341	1340	$\omega$ C-H
60	1365	1372	1365	$\beta$ C-H+ $\delta$ CH <sub>2</sub>
61		1378	1371	$\omega$ CH <sub>2</sub>
62		1416	1411	$\delta$ CH <sub>2</sub>
63		1420	1415	$\delta$ CH <sub>2</sub>
64	1433	1433	1430	$\delta$ CH <sub>2</sub> , $\beta$ N-H
65		1443	1431	$\rho$ N-H
66	1451	1459	1449	$\beta$ C-H (b-ring)+ $\nu$ C-C
67			1456	$\rho$ C-H (p-ring) + $\nu$ C-C
68			1457	$\rho$ C-H (p-ring)
69	1478	1489	1466	$\delta$ CH <sub>2</sub> (p-ring)
70		1576	1574	$\nu$ C-C (b-ring)
71	1605	1604	1597	$\nu$ C-C (b-ring)

72	1619	1649	1649	$\nu$ C=O
73		2731	2728	$\nu$ C-H (p-ring)
74	2737	2736	2733	$\nu$ C-H (p-ring)
75	2797	2805	2805	$\nu_s$ CH <sub>2</sub> (p-ring)
76	2808	2809	2807	$\nu_s$ CH <sub>2</sub> (p-ring)
77	2818	2827	2826	$\nu$ C-H (p-ring)
78	2838	2839	2828	$\nu$ C-H (p-ring)
79	2852	2842	2847	$\nu_{as}$ CH <sub>2</sub> (p-ring)
80		2848	2848	$\nu_{as}$ CH <sub>2</sub> (p-ring)
81	2860	2860	2860	$\nu$ C-H (p-ring)
82	2935	2942	2931	$\nu_{as}$ C-H (b-ring)
83		2948	2940	$\nu_{as}$ C-H (b-ring)
84	2947	2951	2952	$\nu_s$ C-H (b-ring)
85	2962	2995	2994	$\nu_s$ C-H (b-ring)
86	3256	3274	3270	$\nu$ N-H (p-ring)
87	3392	3397	3395	$\nu$ N-H (b-ring)

$\nu$  - stretching;  $\nu_s$  - sym. stretching;  $\nu_{as}$  - asym. stretching;  $\beta$  - in-plane-bending;  $\gamma$  - out-of-plane bending;  $\omega$  - wagging;  $\rho$  - rocking;  $t$  - twisting;  $\tau$  - torsion;  $\delta$  - scissoring.

### NMR analysis

NMR spectroscopy is a sensitive and versatile probe to get faster and easier molecular structural information in solids and liquids. It has an enormous potential for investigating conformations and configurations in organic compounds [33]. The isotropic chemical shifts are frequently used as an aid in identifying reactive organic as well as ionic species [34]. The full geometry of the title compound was performed at DFT/B3LYP/6-311++G(d,p) level for a reliable calculation of its magnetic properties. After optimization, <sup>1</sup>H and <sup>13</sup>C NMR shielding were calculated using the GIAO method [35] by the same level of theory. The isotropic shielding values were used to calculate the isotropic chemical shifts  $\delta$  with respect to the tetramethylsilane (TMS). The value of TMS is 31.88 and 182.46 ppm for <sup>1</sup>H and <sup>13</sup>C respectively. The experimental and calculated <sup>13</sup>C and <sup>1</sup>H NMR data of KBP are reported in Table 2. The calculations reported here were performed in DMSO solution, rather than in the gas phase, using IEF-PCM model. The theoretical chemical shifts have been compared with experimental data and are found to be in compliance with experimental findings. The experimental <sup>1</sup>H and <sup>13</sup>C NMR spectra of the studied compound are presented in Fig. 4 and 5.

There are 12 different carbon atoms for the title molecule. Seven carbon atoms are at the b-ring and the remaining atoms are located in the p-ring. Aromatic carbons give signals in overlapped areas of the spectrum with the chemical shift value ranging from 100 to 150 ppm [36]. The title molecule also falls in the range of literature data. The observed and computed signals of aromatic carbons are in the range of 109.28, 111.79 to 154.15, 158.66 ppm. The chemical shift value of C<sub>7</sub> is higher than the other carbons due to the resonating effect of electronegative oxygen. The chemical shift of C<sub>1</sub> and C<sub>2</sub> are also in the downfield due to the de-shielding effect of the electronegative Nitrogen atoms. The electronegative property of oxygen is higher than the nitrogen atoms causing the chemical shifts value C<sub>7</sub> (158.66 ppm) higher than the other C<sub>1</sub> (133.33 ppm) and C<sub>2</sub> (136.59 ppm). The lowest signal of the methylene carbon atoms observed in C<sub>18</sub> and C<sub>27</sub> in the p-ring.

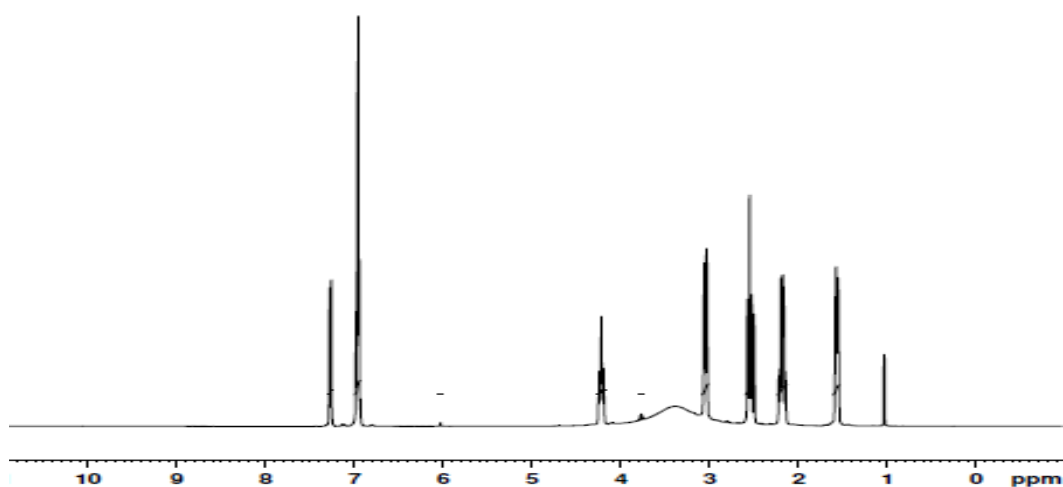


Fig 4. Experimental <sup>1</sup>H NMR spectra of 4-(2-keto-1-benzimidazoliny) piperidine (KBP)

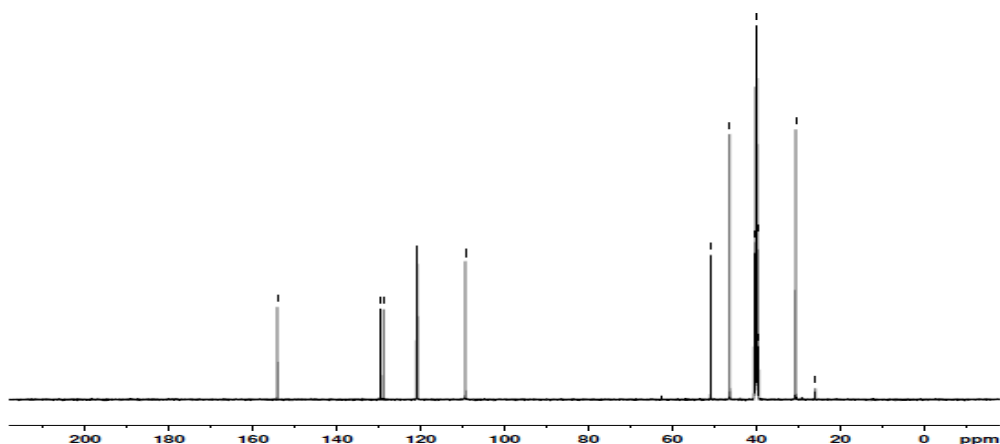


Fig 5. Experimental  $^{13}\text{C}$  NMR spectra of 4-(2-keto-1-benzimidazoliny) piperidine (KBP)

### Proton NMR

In organic molecules, the chemical shifts of aromatic protons are usually observed in the range of 7.00 to 8.00 ppm. The title molecule contains 5 protons in the b-ring and the remaining 10 protons are in the p-ring. The signals of five aromatic protons are observed at 6.96 to 7.29 ppm, calculated at 6.96 to 8.04 ppm. The chemical shift value of H<sub>8</sub> is larger than the other proton signals. The protons in the p-ring were observed in the range of 1.55-4.25 ppm, calculated in the region of 1.59 to 5.01 ppm. The chemical shift value of H<sub>17</sub> is lower than the other protons in the p-ring may be due to the electronegative nature of the nitrogen atom. The observed and calculated value of  $^1\text{H}$  and  $^{13}\text{C}$  NMR show good correlation with each other.

Table 2. Experimental and theoretical  $^1\text{H}$  and  $^{13}\text{C}$  isotropic chemical shift of KBP (with respect to TMS) in DMSO (all values are in ppm)

Atom	Experimental	Calculated	Atom	Experimental	Calculated
H <sub>8</sub>	7.29	8.04	C <sub>7</sub>	154.15	158.66
H <sub>6</sub>	7.25	7.21	C <sub>2</sub>	129.58	136.59
H <sub>10</sub>	6.98	7.17	C <sub>1</sub>	128.79	133.33
H <sub>11</sub>	6.98	7.09	C <sub>5</sub>	120.88	125.29
H <sub>13</sub>	6.96	6.96	C <sub>4</sub>	120.71	124.42
H <sub>31</sub>	4.25	5.01	C <sub>3</sub>	109.36	115.43
H <sub>25</sub>	3.76	3.55	C <sub>6</sub>	109.28	111.79
H <sub>23</sub>	3.74	3.54	C <sub>30</sub>	50.82	47.37
H <sub>26</sub>	3.06	2.97	C <sub>21</sub>	46.28	46.37
H <sub>22</sub>	3.03	2.96	C <sub>24</sub>	46.28	46.28
H <sub>29</sub>	2.49	2.24	C <sub>18</sub>	30.55	33.18
H <sub>19</sub>	2.22	2.23	C <sub>27</sub>	30.55	33.18
H <sub>28</sub>	1.58	1.65			
H <sub>20</sub>	4.57	1.64			
H <sub>17</sub>	1.55	1.59			

### Molecular electrostatic potential (MEP)

Molecular electrostatic potential (MEP) is related to the electronic density and is a very useful descriptor in understanding sites for electrophilic attack and nucleophilic reactions [37,38]. It is related to total charge distribution of the molecule providing the correlations between the molecular properties such as dipole moments, partial charges, chemical reactivity and electronegativity of molecules [39]. The molecular electrostatic potential of the title compound was computed at the B3LYP/6-311++G (d, p) level of DFT and the surface is shown in Figure 6. The electrophilic reactivities are visualized by red colour which indicates the negative regions of the molecule and the positive regions of the molecule are coloured in blue. The carbonyl oxygen atom (O<sub>14</sub>) is surrounded by a greater negative charge surface having the value of -0.05531 a.u., becoming potentially more favourable for electrophilic attacking site, whereas a positive potential indicating the site for nucleophilic attack is concentrated on H<sub>13</sub> atom having the value of -0.05398 a.u.



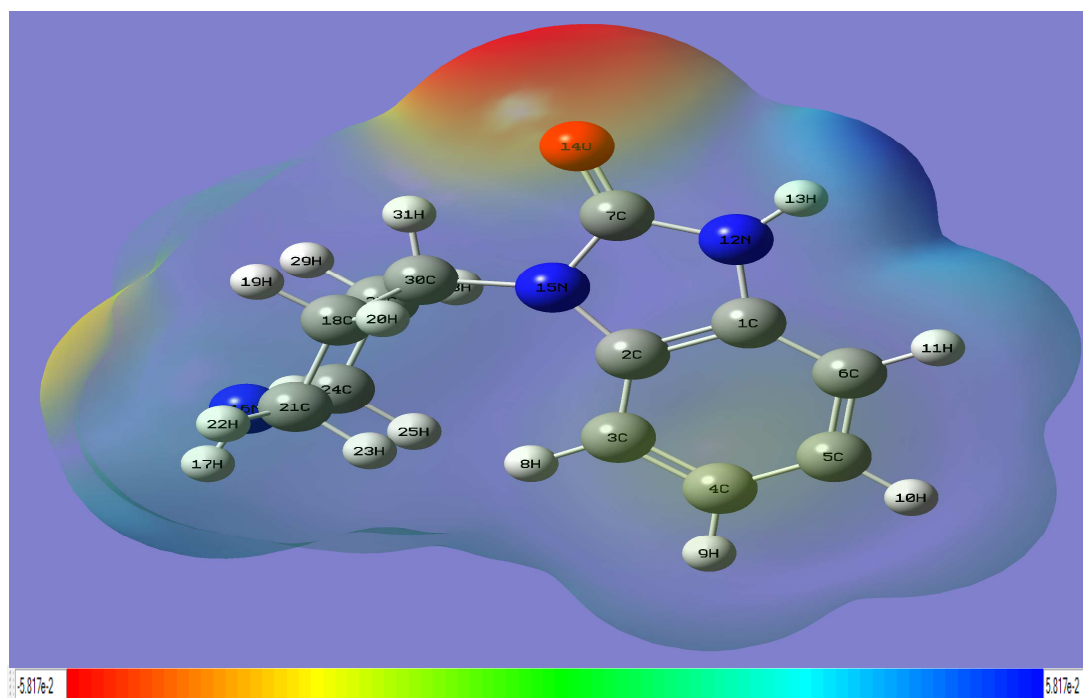
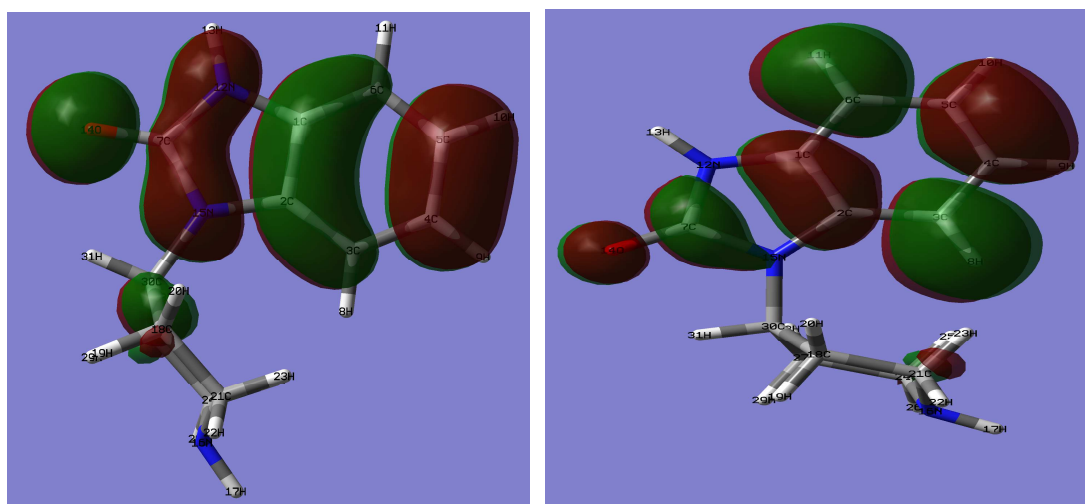


Fig. 6 Molecular electrostatic potential map of 4-(2-keto-1-benzimidazoliny) piperidine (KBP)

#### Frontier Molecular Orbital (FMO) Analysis

The electron densities of the frontier molecular orbitals (FMOs) were used for predicting the most reactive position in  $\pi$ -electron systems and also explained several types of reactions in conjugated system [40]. During molecular interaction, the energy values of the highest occupied molecular orbital ( $E_{\text{HOMO}}$ ), lowest unoccupied molecular orbital ( $E_{\text{LUMO}}$ ) and their energy gap ( $\Delta E$ ) reflect the chemical reactivity of the molecule. Recently, the energy gap between HOMO and LUMO has been used to prove the bioactivity from intra-molecular charge transfer (ICT) [41,42]. The  $E_{\text{HOMO}}$ ,  $E_{\text{LUMO}}$  and  $\Delta E$  values of the studied compound were calculated by B3LYP/6-311++G(d,p) method and the HOMO and LUMO pictures are shown in Figure 7.



HOMO of KBP

LUMO of KBP

Fig. 7 Atomic orbital composition of the frontier molecular orbital for KBP

#### Global reactivity descriptors

The widely used global reactivity indices like, global hardness( $\eta$ ), global softness( $S$ ), electronegativity( $\chi$ ) and chemical potential( $\mu$ ) and electrophilicity index( $\omega$ ) are used to understand the global nature of molecules in terms of their stability and also it is possible to gain knowledge about the reactivity of molecules. The calculated global reactivity descriptors values of KBP are tabulated in table 3. According to the Koopman's theorem [43] ionization potential ( $I$ ) and electron affinity ( $A$ ) can be expressed as follows in terms of  $E_{\text{HOMO}}$ ,  $E_{\text{LUMO}}$  the highest occupied molecular orbital energy, and the lowest unoccupied molecular orbital energy, respectively



$$I = -E_{\text{HOMO}} \quad (1)$$

$$A = -E_{\text{LUMO}} \quad (2)$$

When the values of  $I$  and  $A$  are known, the values of the absolute electronegativity  $\chi$ , and the absolute hardness  $\eta$  can be determined through the following expressions [44]

$$\chi = \frac{I + A}{2} \quad (3)$$

Chemical hardness ( $\eta$ ) is obtained from the equation:

$$\eta = \frac{I - A}{2} \quad (4)$$

It measures the resistance of an atom to a charge transfer. Electronegativity and hardness have proved to be very useful quantities in the chemical reactivity theory.

The chemical potential  $\mu$ , the negative of electronegativity ( $\chi$ ) of a system is useful for describing phase transitions, the stratification of gases in a gravitational field, electric currents in semi-conductor junctions and nuclear reactions [45]. It can be obtained by the following equation [46].

$$\mu = -\frac{I + A}{2} \quad (5)$$

Compounds having greater values of chemical potential are most reactive than one with small electronic chemical potential

The electrophilicity index ( $\omega$ ), has become a powerful tool for the study of the reactivity of organic molecules participating in polar reactions [47]. It measures the favourable change in energy when a chemical system attains saturation by addition of electrons and is calculated by the equation

$$\omega = \frac{\mu^2}{2\eta} \quad (6)$$

A good electrophile is a species characterised by a high ( $\omega$ ) value and a low ( $\eta$ ) value.

**Table 3. HOMO LUMO energy value and related quantum chemical parameters of KBP calculated by B3LYP/6-311++G(d,p) method.**

Parameter	Energy(eV)
$E_{\text{HOMO}}$ (eV)	-5.905
$E_{\text{LUMO}}$ (eV)	-0.639
Energy gap( $\Delta E$ )	5.266
Dipole moment ( $\mu$ in Debye)	3.2683
Hardness( $\eta$ )	2.633
Electronegativity( $\chi$ )	3.272
Softness ( $S$ )	0.379
Electrophilicity index( $\omega$ )	2.033
Chemical potential( $\mu$ )	-3.272

### Local reactivity descriptors

The Fukui function is a local reactivity descriptor that indicates the preferred regions where a chemical species will change its density when the number of electrons is modified [48,49]. It allows determining the pin point distribution of the active sites on a molecule. The regions of a molecule where the Fukui function is large are chemically softer than the regions where the Fukui function is small. However, for studying the reactivity at the atomic level, a more convenient way of calculating the Fukui function is through the condensed forms of the Fukui function for an atom  $k$  in a molecule which are expressed as: [48]

$$f_k^+ = q_{\text{N}+1} - q_{\text{N}} \quad \text{for nucleophilic attack} \quad (1)$$

$$f_k^- = q_{\text{N}} - q_{\text{N}-1} \quad \text{for electrophilic attack} \quad (2)$$

where  $q_{\text{N}}$ ,  $q_{\text{N}+1}$  and  $q_{\text{N}-1}$  are the electronic population of the atom  $k$  in neutral, anionic and cationic systems.

The local softness  $s$ , for an atom can be expressed as the product of the condensed Fukui function( $f$ ) and the global softness( $S$ ) as follows [50]

$$s^+ = (f^+) S \quad (3)$$

$$s^- = (f^-) S \quad (4)$$

The local softness as like those obtained from the condensed Fukui function also have the additional information about the total molecular softness, which is related to the global reactivity with respect to the reactive agents. A high value of  $s^+$  indicates high nucleophilicity and a high value of  $s^-$  high electrophilicity.

Fukui and local softness indices for nucleophilic and electrophilic attack of the title molecule is reported in table 4. It was observed that, the more reactive site for nucleophilic attack takes place on H<sub>11</sub> atom and the more reactive site for electrophilic attack on O<sub>14</sub> atom.

**Table 4. Fukui and local softness indices for nucleophilic and electrophilic attacks in KBP atoms calculated from Mulliken atomic charges ; Maxima in bold**

Atom No	$f_k^+$	$f_k^-$	$s_k^+$	$s_k^-$
1 C	0.09196	-0.01103	0.04950	-0.00594
2 C	0.21589	-0.04641	0.11623	-0.02498
3 C	0.54624	0.05173	0.29407	0.02785
4 C	-1.03296	0.02090	-0.55610	0.01125
5 C	-1.22238	0.01408	-0.65808	0.00758
6 C	-0.15452	0.06159	-0.08318	0.03316
7 C	-0.12648	0.00880	-0.06809	0.00473
8 H	-0.32413	0.05798	-0.17449	0.03121
9 H	0.57777	0.06134	0.31104	0.03302
10 H	0.29622	0.06759	0.15947	0.03639
11 H	<b>1.21819</b>	0.05632	<b>0.65582</b>	0.03031
12 N	-0.04219	0.04937	-0.02271	0.02658
13 H	0.46629	0.04649	0.25103	0.02503
14 O	0.03448	<b>0.15008</b>	0.01856	<b>0.08079</b>
15 N	-0.05700	0.05824	-0.03068	0.03135
16 N	-0.39256	0.00092	-0.21133	0.00049
17 H	0.49588	0.05563	0.26696	0.02994
18 C	0.13511	-0.04013	0.07274	-0.02160
19 H	0.03948	0.03833	0.02125	0.02063
20 H	0.07954	0.02487	0.04282	0.01338
21 C	-0.86478	0.05246	-0.46556	0.02824
22 H	0.53562	0.04160	0.28835	0.02239
23 H	0.32298	0.01519	0.17387	0.00817
24 C	-0.86403	0.00772	-0.46515	0.00415
25 H	0.32358	0.03059	0.17420	0.01647
26 H	0.53609	0.03939	0.28861	0.02121
27 C	0.13361	0.00439	0.07193	0.00236
28 H	0.079523	0.01964	0.04281	0.01057
29 H	0.039387	0.03950	0.02120	0.02126
30 C	-0.546936	-0.00682	-0.29445	-0.00367
31 H	0.013751	0.02963	0.00740	0.01595

## CONCLUSION

In this study, FT-IR, FT-Raman and NMR spectra of 4-(2-keto-1-benzimidazolynyl) piperidine (KBP) were studied. The optimized molecular structure, vibrational and electronic properties of the title compound have been calculated by DFT method B3LYP using 6-311++G(d,p) basis set. The observed wavenumbers are found to be in agreement with the theoretically calculated values. The experimental and calculated spectra are in good agreement. The molecular electrostatic potential (MEP), HOMO and LUMO level analyses as well as global reactivity descriptors were discussed. Fukui function also helps to identify the electrophilic/nucleophilic nature of a specific site within a molecule.

## REFERENCES

- [1] A.Aejaz , K.I.Molvi, N.Sayed , B.Irshad , M.Tausif ,R.Memon R, *J. Chem. Pharma. Res.*, **2012**, 4, 872.
- [2] H.Khalid, Aziz-ur-Rehman, M.A.Abbasi, K.M. Khan, *Inter. J. Pharm. Pharmace. Sci.*, **2012**, 3, 443.
- [3] K.M.Khan, Z.S.Saify, M.A.Lodhi, N.Butt, S.Perveen , G.M.Maharvi, M.I.Choudhary, Atta-ur-Rahman, *Nat. Prod. Res.*, **2006**, 20, 523.
- [4] P.S.Watson, B.Jiang, B. Scott, *Org. Lett.*, **2000**, 2, 3679.

- [5] T. Klockgether, U. Wullner, J. P. Steinbach, V. Petersen, L. Turski and P.Loschmann, *Eur. J. pharmacol.*, **1996**, 301, 67.
- [6] W. E. Meyer, A. S. Tomcufcik, P. S. Chan, and M. Haug, *J. Med. Chem.*, **1989**, 32, 593.
- [7] F.J.Janssens, Torremans, P.A.Janssen, *J. Med.Chem.*, **1986**, 29, 2290.
- [8] M.K. Subramanian, P.M. Anbarasan, S. Manimegalai, *J. Raman Spectrosc.*, **2009**, 40 1657.
- [9] S. Sebastian, N. Sundaraganesan, *Spectrochim. Acta Part A*, **2010**, 75, 94.
- [10] Yasser Karzazi1, Mohammed El Alaoui Belghiti, Ali Dafali and Belkheir Hammouti, *J. Chem. Pharm. Res.*, **2014**, 6(4),689.
- [11] Amina Mirsakiyeva, Darya Botkina, Karim Elgammal, Assel Ten, Hakan W. Hugosson, Anna Delin and Valentina Yue, *ARKIVOC*, **2016**, (iv), 86.
- [12] K.Kalaiselvi, A.Kavithamani, *Res. J. Chem. Sci.*, **2014**, 4(12), 7.
- [13] M. J. Frisch et al., Gaussian 09, Revision A. 9, Gaussian, Inc., Pittsburgh, **2009**.
- [14] H.B. Schlegel, *J. Comput. Chem.*, **1982**, 3, 214.
- [15] N.Sundaraganesan, S.Ilakiamani, H.Saleem, P.M.Wojciechowski, D.Michalska, *Spectrochim. Acta A*, **2005**, 61, 2995.
- [16] K. Wolinski, R. Haacke, J.F. Hinton, P. Pulay, *J. Comp. Chem.*, **1997** 18 (6), 816.
- [17] M. Rohlfing, C. Leland, C. Allen, R. Ditchfield, *Chem. Phys.*, **1984**, 87, 9.
- [18] Y.Erdogdu, M.T.Gulluoglu, *Spectrochim Acta A*, **2009**, 74, 162.
- [19] M.T.Gulluoglu, Y.Erdogdu and S.Yurdakul, *J.Mol.Struct*, **2007**, 834, 540.
- [20] A.Altun, K.Golcuk, M.Kumru, *J. Mol. Struct.*, **2003**, 155, 637.
- [21] S. Saravanan, V. Balachandran, K. Viswanathan, *Spectrochim. Acta Part A, Mol. Biomol. Spectrosc.*, **2014**, 121, 685.
- [22] N. Sundaraganesan, S.Illakiamani, C.Meganathan, B.Joshua, *Spectrochim. Acta Part A*, **2007**, 67, 214.
- [23] A.Thirunavukkarasu, R.Karunathan, J.Mallika and V.Sathyarayanmoorthi, *Ind.J.Pure and Appl. Phys.*, **2014**, 52, 653.
- [24] D. Sajan, J.Binoy, B.Pradeep K.V.Krishnan, V.B Kartha I.H.Joe, V.S.Jayakumar, *Spectrochim Acta A*, **2004**, 60, 173.
- [25] D.B. Powell, *Spectrochim Acta*, **1960**, 16, 241.
- [26] B.S Yadav, Israt Ali, Pradeep kumar, Preeti Yadav, *Ind. J. pure and Appl. Phys.*, **2007**, 45, 979.
- [27] Satish Chand, Shilendra K Pathak, Alok K Sachan, Ruchi Srivastava, Vikas K Shukla; V .Narayan, A.Kumar, Onkar Prasad, Leena Sinha, *J. Chem. Pharm.Res.*, **2014**, 6(3), 1434.
- [28] I. Lopez-Tocon, M. Becucci, G. Pietraperzia, E. Castellucci, J.C. Otero, *J. Mol. Struct.*, **2001**, 565, 421.
- [29] N.P.G. Roeges, *A Guide to the Complete Interpretation of Infrared Spectra of Organic Structures*, Wiley, New York, **1994**.
- [30] G. Socrates, *Infrared Characteristic Group Frequencies*, John Wiley and Sons, New York **1981**.
- [31] E. Tatsch, B. Schrader, *J. Raman Spectrosc.*, **1995**, 26, 467.
- [32] G. A. Neville, H. F. Shurvell, *J. Raman Spectrosc.*, **1990**, 21, 9.
- [33] R.H Contreras, J.E. Peralta, *Prog. Nucl. Magn. Reson. Spectrosc.* **2000**, 37, 321.
- [34] Sirukarumbur Panduranga Vijaya Chamundeeswari, Emmanuel Rajan James Jebaseelan Samuel and Namadevan Sundaraganesan, *European Journal of Chemistry*, **2011** 2 (2), 136.
- [35] R. Ditchfield, *Mol. Phys.*, **1974**, 27, 789.
- [36] H.O. Kalinowski, S. Berger, S. Braun, *Carbon-13 NMR spectroscopy*, John Wiley & Sons, Chichester, **1988**.
- [37] E.Scrocco, J.Tomasi, *Adv. Quantum Chem.* **1978**, 11, 115.
- [38] F.J Luque, J.M. Lopez, M.Orozco, *Theor. Chem. Acc.*, **2000**, 103, 343.
- [39] J.S. Murray, K.Sen, *Molecular Electrostatic Potentials, Concepts and 399 Applications*, Elsevier, Amsterdam, **1996**.
- [40] K.Fukui, T.Yonezawa, H.J.Shingu, *J. Chem. Phys.* **1952**, 20, 722.
- [41] L. Padmaja, C.Ravikumar, D.Sajan, I.H. Joe, V.S.Jayakumar, G.R. Pettit, F.O.Neilsen, *J. Raman Spectrosc* **2009**, 40, 419.
- [42] C.Ravikumar, I.H.Joe, V.S.Jayakumar, *Chem. Phys. Lett.* **2008**, 460, 552.
- [43] T.Koopmans, *Physica*, **1933**, 1, 104.
- [44] L.Pauling, *J. Am. Chem. Soc.*, **1932**, 54, 3570.
- [45] G.Frenking, A.Krapp, *J. Comput. Chem.*, **2007**, 28, 15.
- [46] R.G.Parr, R.G Pearson, *J. Am. Chem. Soc.* **1983**, 105, 7512.
- [47] P.Perez, L.R.Domingo, A.Aizman, R.Contreras, *The Electrophilicity Index in Organic Chemistry in Theoretical Aspects of Chemical Reactivity*; Elsevier: New York, NY, USA, Volume 19, **2007**.
- [48] W. Yang, W.J.Mortier, *J. Am. Chem. Soc.*, **1986**, 108, 5708.
- [49] P. Fuentealba, P.Perez, R.Contreras, *J. Chem. Phys.*, **2000**, 113, 2544
- [50] S.R. Stoyanov, S. Gusarov, S.M. Kuznick, A. Kovalenko, *Mol.Simul.*, **2008**, 34, 943.